



XXIV Italian Group of Fracture Conference, 1-3 March 2017, Urbino, Italy

Duplex stainless steels “475°C embrittlement”: influence of the chemical composition on the fatigue crack propagation

Vittorio Di Cocco^{a*}, Francesco Iacoviello^a, Gloria Ischia^b

^aUniversità di Cassino e del Lazio Meridionale, DICeM, via G. Di Biasio 43, 03043, Cassino (FR), Italy

^bUniversità di Trento, DII, via Sommarive, 9, 38123 Povo, Trento, Italy

Abstract

Duplex stainless steels (DSSs) are prone to age hardening and embrittle over a wide temperature range depending on their chemical composition. This is mainly due to precipitation phenomena that may occur inside ferrite grains and at ferrite-austenite grain boundaries. The aim of this work is the analysis of chemical composition influence on fatigue crack propagation resistance of “475°C embrittled” duplex stainless steels. Fatigue crack propagation resistance of 21 Cr 1 Ni, 22 Cr 5 Ni and 25 Cr 7 Ni duplex stainless steels was investigated considering both as received and 475°C embrittled conditions (1000h). Microstructural analyses were performed using a transmission electron microscope (TEM). Concentrations of the main elements, but carbon, were evaluated using a standardless analysis program.

Copyright © 2017 The Authors. Published by Elsevier B.V. This is an open access article under the CC BY-NC-ND license (<http://creativecommons.org/licenses/by-nc-nd/4.0/>).

Peer-review under responsibility of the Scientific Committee of IGF Ex-Co.

Keywords: 475°C embrittlement; TEM analysis; Fatigue crack propagation.

1. Introduction

Duplex stainless steels are successfully used in chemical, petrochemical, nuclear, fertilizer and food industries. Their good mechanical properties and their excellent corrosion resistance in many environments and operating conditions, like chloride induced stress corrosion, mainly depend on their chemical composition and on the ferrite and austenite volume fractions, Lacombe (1990), Gunn (1997), Iacoviello (2005). Considering the pitting index, or pitting resistant equivalent (e.g. $PRE = \%Cr + 3.3 (\%Mo + 0.5\%W) + 16 \%N$), these steels can be classified considering three classes at least:

* Corresponding author. Tel.: +39.67762994334.

E-mail address: v.dicocco@unicas.it

- “lean” duplex: they are characterized by a PRE value that is about 25, with very low Mo and Ni content; they can be considered as valid substitute of AISI 304;
- “standard” duplex steel: having a PRE values of about 35, 22 Cr 5 Ni DSS can be considered as the standard alloy.
- “superduplex” stainless steels: having PRE values greater than 40; they are characterized by a corrosion resistance.

Depending on their chemical composition, these steels are prone to age hardening and embrittlement over a wide temperature range. This is mainly due to precipitation phenomena that may occur inside ferrite grains and at ferrite-austenite grain boundaries, Charles (2000) and Iacoviello (2005).

Three different critical temperatures ranges are present:

- Between 300 and 600°C. This temperature range is characterized by the spinodal decomposition of ferrite into Cr-poor α and Cr-rich α' domains. Other precipitation processes would also occur. Among them, the main one is the Ni, Si, Mo-rich G phase precipitation, Guttman (1991), Iacoviello (2005) and Danoix (2000). These particles are very small (usually from 1 to 10 nm, occasionally up to 50 nm) and they precipitate, more or less uniformly, within the ferrite grains, depending on the actual chemical composition of the steel (e.g. Mo-bearing steels show a more uniform precipitation than Mo-free steels). However, these particles are shown to form preferentially on dislocations and at α - γ interfaces. Their composition depends not only on the steel composition, but also on the ageing conditions. For instance, the overall concentration in G-forming elements increases from 40 to 60% if tempered at 350°C respectively for 1000 and 30000 hours.

- Between 600 and 1050°C. This critical temperature range is characterized by the formation, both inside austenite and ferrite, of a variety of secondary phases that may precipitate with incubation times that are strongly affected by the chemical composition, Nilsson (1992): σ phases, nitrides (Cr_2N , π), secondary austenite, χ and R phases, carbides (M_7C_3 , M_{23}C_6). The precipitation of these carbides, nitrides and secondary phases strongly influences mechanical properties and corrosion resistance of duplex stainless steels, Iacoviello (1997, 1998 and 1999).

- Above 1050°C. Duplex stainless steels, that have a fully ferritic solidification structure, upon cooling, partly transform into austenite. This transformation is reversible: therefore, any temperature increase above 1050°C implies a ferrite volume fraction increase and a decrease in the partition coefficients of the alloying elements, Charles (2008).

The first critical temperature range implies a limited long-time service temperature, usually lower than 350°C (inlet temperature in some duplex stainless steels heat exchanger, Fruitier (1991)). In this work, chemical composition influence on DSS “475°C embrittlement” phenomenon has been investigated both considering fatigue crack propagation resistance and analyzing microstructure transformations using a transmission electron microscope (TEM). Three different rolled DSS were investigated considering the same ferrite/austenite ratio (Tabs. 1-3).

Table 1: 21 Cr 1 Ni “lean” DSS chemical composition (wt%) and tensile properties (PRE = 26); EN 1.4162.

C	Mn	Cr	Ni	Mo	N
0.03	5.00	21.5	1.5	0.3	0.22
YS [MPa]	UTS [MPa]	A%			
483	700	38			

Table 2: 22 Cr 5 Ni DSS chemical composition (wt%) and tensile properties (PRE = 35); EN 1.4462.

C	Mn	Cr	Ni	Mo	N
0.019	1.51	22.45	5.50	3.12	0.169
YS [MPa]	UTS [MPa]	A%			
565	827	35			

Table 3: 25 Cr 7 Ni superduplex stainless steel (SSS) chemical composition (wt%) and tensile properties (PRE = 42); EN 1.4410.

C	Mn	Cr	Ni	Mo	N
0.019	0.80	24.80	6.80	3.90	0.30
YS [MPa]	UTS [MPa]	A%			
556	814	31			

2. Investigated steels and experimental procedures

Investigated rolled stainless steels chemical composition and tensile properties are shown in tables 1-3. All the investigated steels are characterized by the same ferrite/austenite ratio ($\alpha/\gamma = 1$) and show the rolling texture as in Fig. 1.

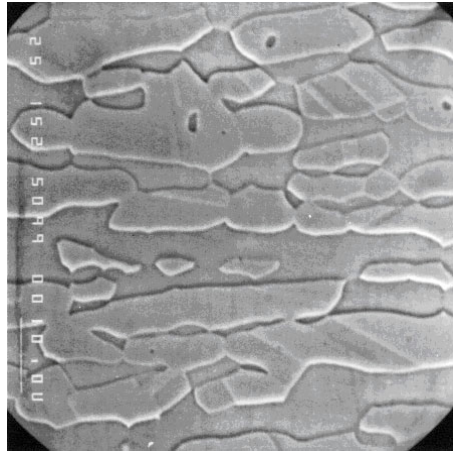


Fig. 1: 22 Cr 5 Ni DSS microstructure (SEM; electrochemical etching in oxalic acid – $(\text{COOH})_2$ 3V – 60 s).

Fatigue crack propagation tests were run according to ASTM E647 standard (2015), using 10 mm thick CT (Compact Type) specimens and considering three different stress ratio values ($R = P_{\min}/P_{\max} = 0.1; 0.5; 0.75$). Tests were performed using a computer controlled servohydraulic machine in constant load amplitude conditions (sinusoidal loading waveform) at room temperature, with a loading frequency of 30 Hz. Crack length measurements were performed by means of a compliance method using a double cantilever mouth gage. All the steels were investigated considering the following heat treatments:

- solution annealed 1050°C for 1 h (as received);
- 475°C for 1000 h.

Scanning electron microscope (SEM) fracture surface analysis was performed, in order to identify the main fatigue crack propagation micromechanisms.

Microstructural analyses were performed using a transmission electron microscope (TEM). Thin foils for TEM observations were prepared by a preliminary mechanical thinning, down to 100 μm thickness, followed by twin-jet polishing in a solution of 2-butoxiethanol (90%) and perchloric acid (10%) at $-3 \div -1^\circ\text{C}$, using a voltage of 20-35V depending the composition of the steel. Observations were performed with an analytical instrument operated at 120 kV, using a double-tilt sample holder for a more efficient acquisition of selected area electron diffraction (SAED) patterns. TEM was equipped with an energy dispersive x-ray spectrometer (EDXS). Concentrations of the main elements, but carbon, were evaluated using a standardless analysis program.

3. Results and discussion

Due to the high fatigue crack propagation tests repeability in DSS, Iacoviello (2000), only one fatigue test will be considered for all the investigated steels and heat treatments. For all the investigated duplex stainless steels, “475°C embrittlement” and stress ratio influence are shown in Figs. 2-4.

Solubilized 22Cr 5 Ni and 25 Cr 7 Ni are characterized by the same fatigue crack propagation resistance, whereas 21 Cr 1 Ni stainless steel shows crack growth rates that are up to four times higher, for the same loading conditions (R and applied ΔK). The influence of the 475°C embrittlement heat treatment is strongly affected by the steel chemical composition:

- 21 Cr 1 Ni (Fig. 2): crack growth rates that are substantially unchanged if compared to the solubilized steel for all the investigate R values (Fig. 2); embrittlement degree is practically negligible;

- 22 Cr 5 Ni (Fig. 3): stage I (threshold stage) is substantially unchanged, whereas stage II (Paris stage) is characterized by a higher slope, with crack growth rates increase that becomes more and more evident with the increase of the applied ΔK and/or the R value;

- 25 Cr 7 Ni (Fig. 4): applied ΔK threshold values (ΔK_{th}) clearly decrease and crack growth rates are higher than the values obtained with the solubilized steel, but differences do not increase with the applied ΔK as in 22 Cr 5 Ni.

Fracture surface SEM analysis confirms differences in 475°C embrittlement influence in the investigated duplex stainless steels (Figs. 5-10; cracks growth from left to right).

21 Cr 5 Ni stainless steel is characterized by the presence of striation for all the investigated loading conditions and, corresponding to high R and/or ΔK values, to ferrite grain cleavage. The relative importance of these two morphologies is substantially unchanged from the solubilized steel to the 475°C embrittled one (Figs. 5 and 6).

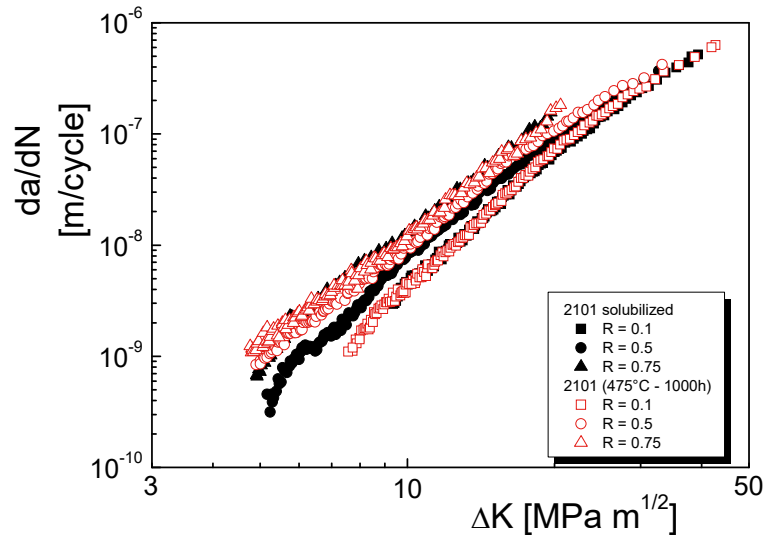


Fig. 2: 475°C embrittlement influence on 21 Cr 1 Ni stainless steel fatigue crack propagation resistance (R = 0.1; 0.5; 0.75).

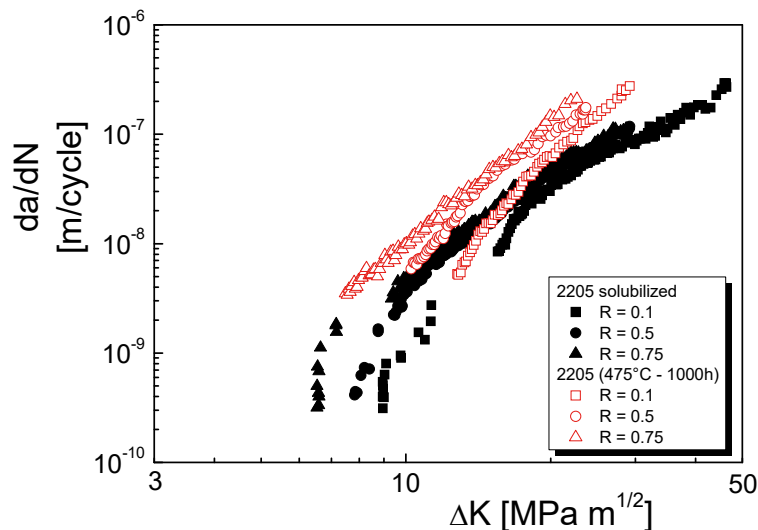


Fig. 3: 475°C embrittlement influence on 22 Cr 5 Ni stainless steel fatigue crack propagation resistance (R = 0.1; 0.5; 0.75).

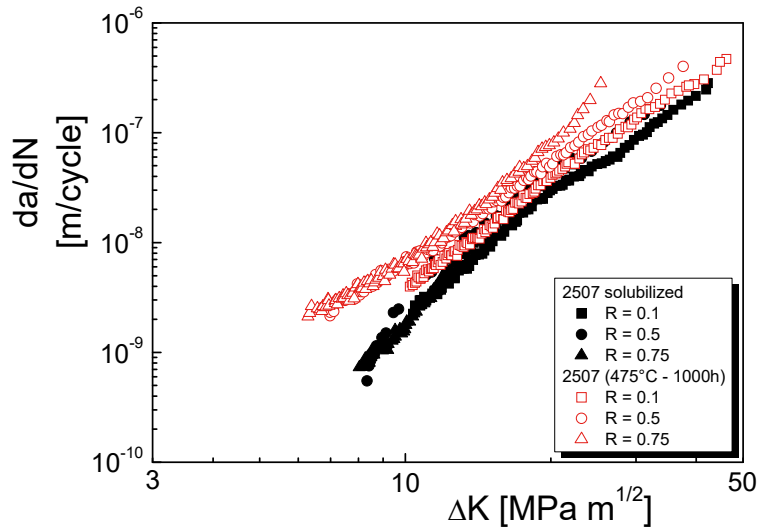


Fig. 4: 475°C embrittlement influence on 25 Cr 7 Ni stainless steel fatigue crack propagation resistance (R = 0.1; 0.5; 0.75).

22 Cr 5 Ni stainless steel fracture surfaces are not influenced for lower R and/or ΔK value, but they clearly change in the stage II of III of crack propagation (Paris stage), where the main fatigue crack propagation micromechanism (ductile striations both in austenite and in ferrite grains, Fig. 7) clearly changes. Corresponding to ferritic grains, cleavage and fragile striation become more and more evident with the increase of the applied ΔK (Fig. 8).

Finally, 475°C embrittled 25 Cr 7 Ni stainless steel is characterized by an evident ferrite grains cleavage, also corresponding to low ΔK values (Figs. 9 and 10). The increase of the applied ΔK implies a more fragile fracture surface morphology, with the presence of really evident secondary cracks, mainly transgranular, but also partially intergranular.

Considering that all the investigated DSS are characterized by the same ferrite/austenite ratio ($\alpha/\gamma = 1$) and by analogous heat treatments, differences in the macroscopic fatigue crack propagation resistance (Fig. 2-4) and in the fatigue crack propagation micromechanisms should be investigated considering the chemical composition influence on ferrite spinodal decomposition and on secondary phases precipitation at 475°C.

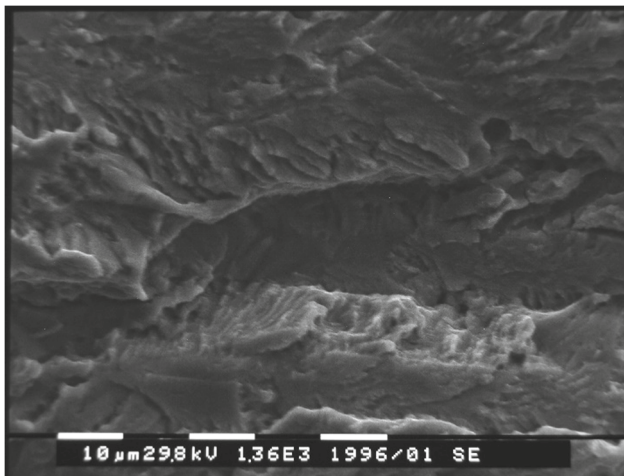


Fig. 5: Solubilized 21 Cr 1 Ni DSS fracture surface ($\Delta K = 15 \text{ MPa}\sqrt{\text{m}}$, R=0.1).

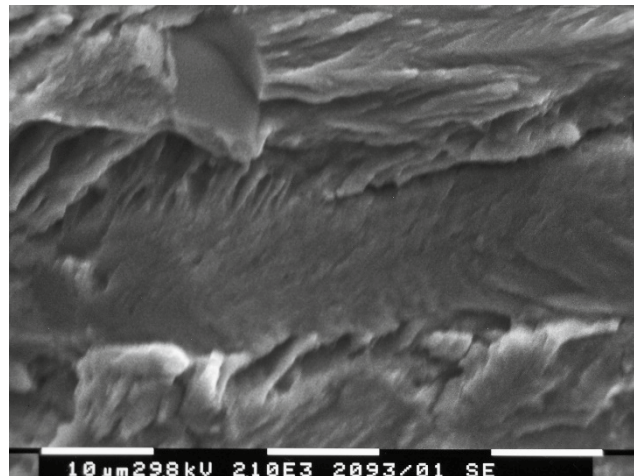


Fig. 6: 475°C embrittled 21Cr 1 Ni DSS fracture surface ($\Delta K=15 \text{ MPa}\sqrt{\text{m}}$, R=0.1).

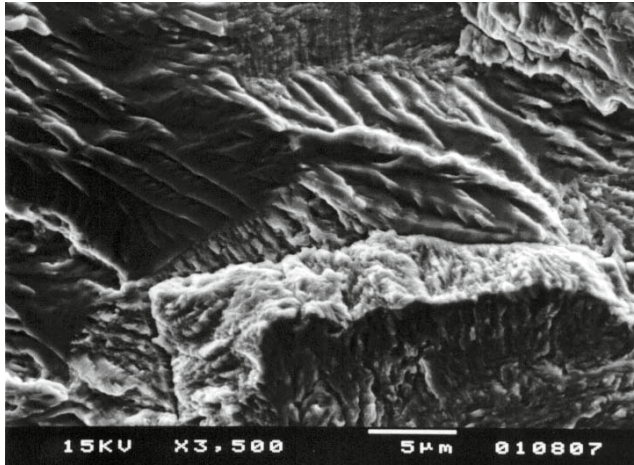


Fig. 7: Solubilized 22 Cr 5 Ni DSS fracture surface ($\Delta K = 20 \text{ MPa}\sqrt{\text{m}}$, $R = 0.1$).

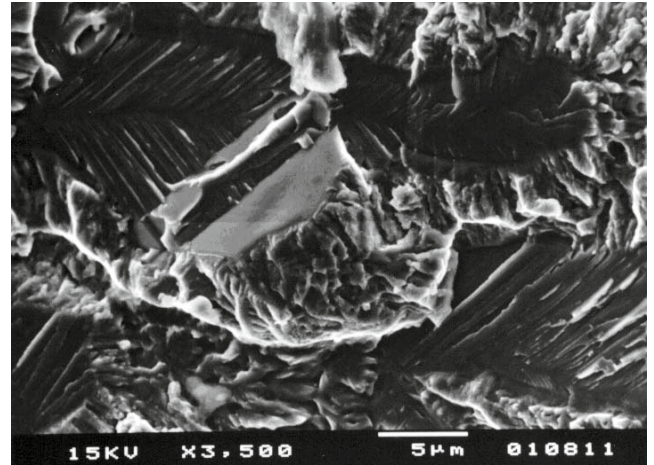


Fig. 8: 475°C embrittled 22 Cr 5 Ni DSS fracture surface ($\Delta K = 20 \text{ MPa}\sqrt{\text{m}}$, $R = 0.1$).

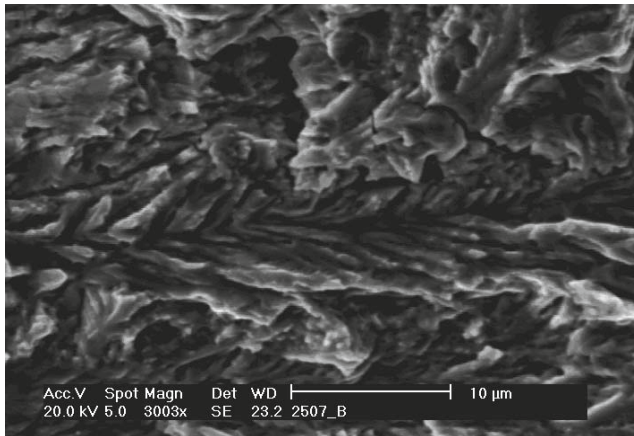


Fig. 9: Solubilized 25 Cr 7 Ni DSS fracture surface ($\Delta K = 20 \text{ MPa}\sqrt{\text{m}}$, $R = 0.1$).

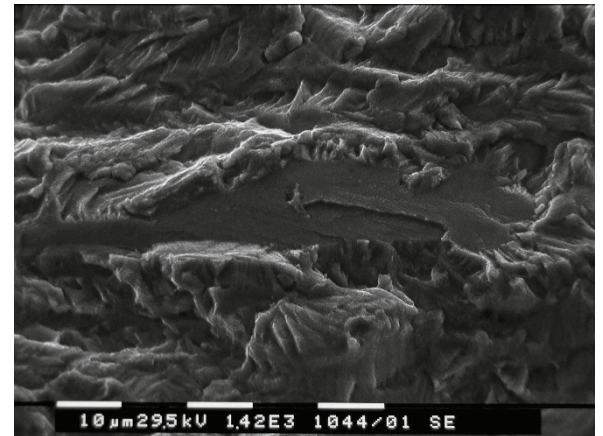


Fig. 10: 475°C embrittled 25 Cr 7 Ni DSS fracture surface ($\Delta K = 20 \text{ MPa}\sqrt{\text{m}}$, $R = 0.1$).

Considering that optical observation or SEM observation are not able to display any microstructural modifications due to 475°C tempering heat treatment, TEM observations were performed more successfully.

21 Cr 1 Ni DSS showed some precipitates corresponding to the ferritic grain, with visible dislocation lines piled up to the grain boundaries (Fig. 11) and inside ferritic grains (Fig. 12). Also 22 Cr 5 Ni DSS is characterized by the same dislocation distribution in ferritic grains (inside and at grain boundaries) and some dislocation lines display a pinned structure: considering that any other reflection than those of the body centered cubic cell were not obtained, this probably indicate that G phase precipitation has actually started, but it is still at too an early stage (Fig. 13). Furthermore, considering a higher magnification image (Fig. 14), it is possible to see a slightly modulated contrast, that could be due to the early stages of the spinodal decomposition of ferrite into α and α' phases, Park (2002). They both have a body centered cubic (bcc) structure, with a very similar parameter and thus retain coherent interfaces.

Ferritic grains in 475°C tempered 25 Cr 7 Ni DSS are characterized by homogeneously distributed precipitates (Fig. 15) that are characterized by a curly aspect, probably due to their preferential nucleation sites (dislocation lines, Fig. 16). G phase is characterized by a lattice parameter that is about four times larger than ferrite lattice parameter, but, as for the two other investigated DSS, no extra spots were detected in any of the acquired diffraction

pattern, probably due to the very low volume fraction of these precipitates.

As a consequence of the TEM analysis performed on the 475°C tempered DSS and SSS, it is possible to point out that after 1000 hours:

- spinodal decomposition is only scarcely developed and is not clearly evident for all the investigate stainless steel;
- G phase precipitation is more and more developed with the content increase of G phase forming elements (mainly Ni, Mo).

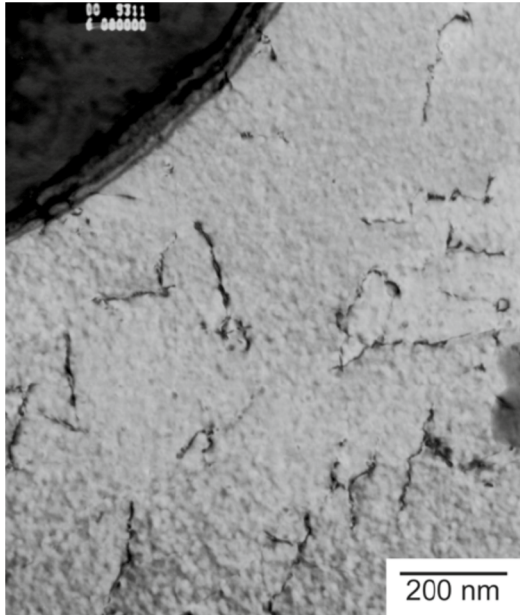


Fig. 11: 475°C – 1000 h tempered 21 Cr 1 Ni DSS microstructure TEM analysis; dislocations at ferritic grain boundary.

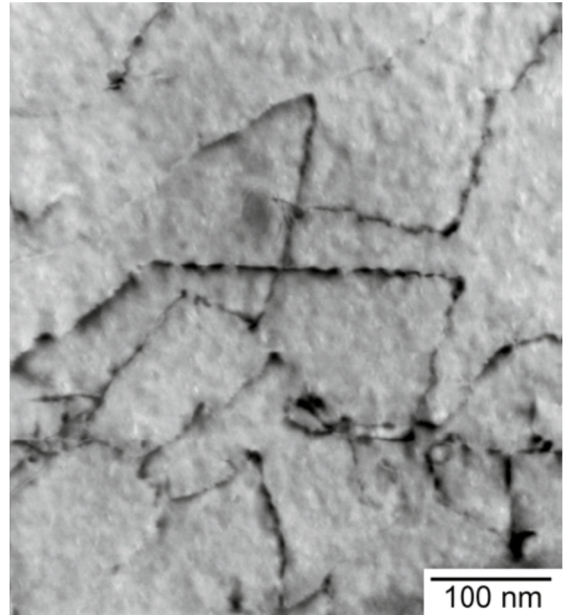


Fig. 12: 475°C – 1000h tempered 21 Cr 1 Ni DSS microstructure TEM analysis; dislocations in ferritic grain.

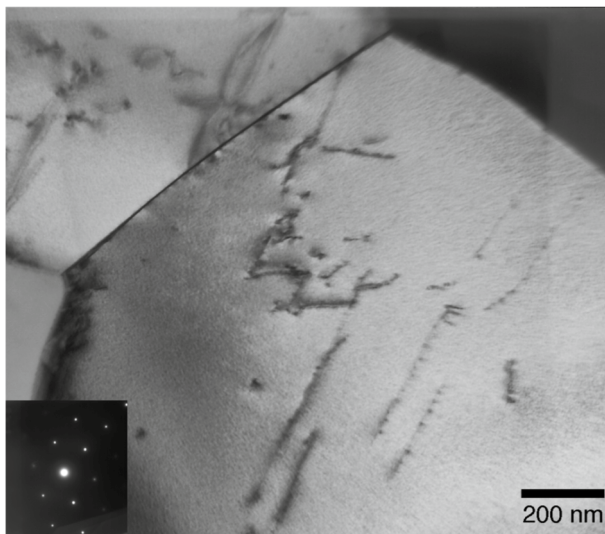


Fig. 13: 475°C – 1000 h tempered 22 Cr 5 Ni DSS microstructure TEM analysis. Bright field image and selected area diffraction pattern for $\langle 111 \rangle$ zone axis.

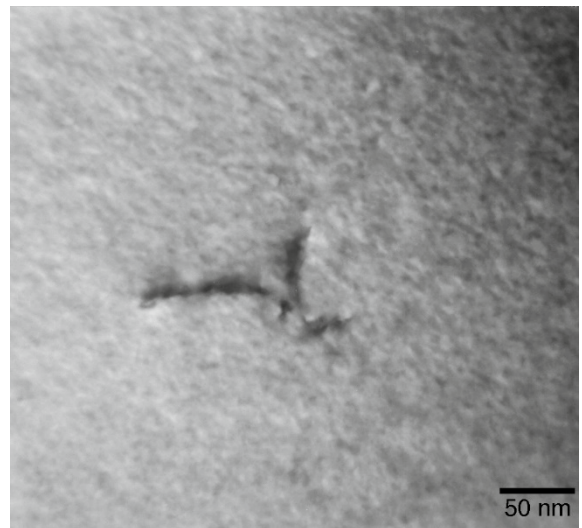


Fig. 14: 475°C – 1000 h tempered 22 Cr 5 Ni DSS microstructure TEM analysis. TEM bright field image of a dislocation in a ferritic region imaged along $\langle 110 \rangle$ direction.

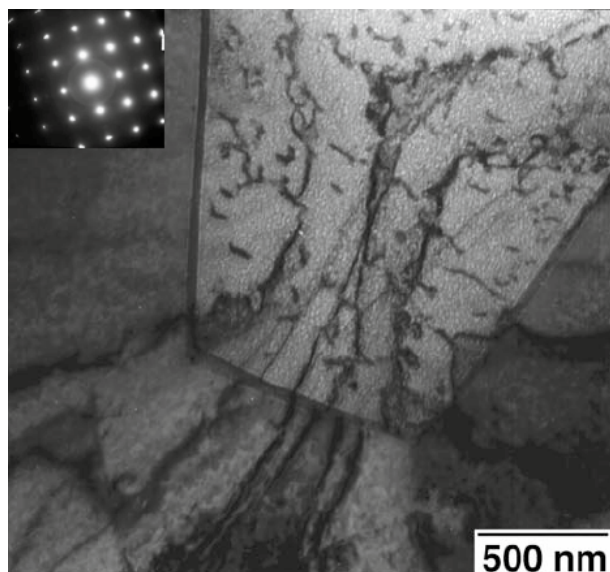


Fig. 15: 475°C – 1000 h tempered 25 Cr 7 Ni DSS microstructure TEM analysis; ferritic grain with precipitates.

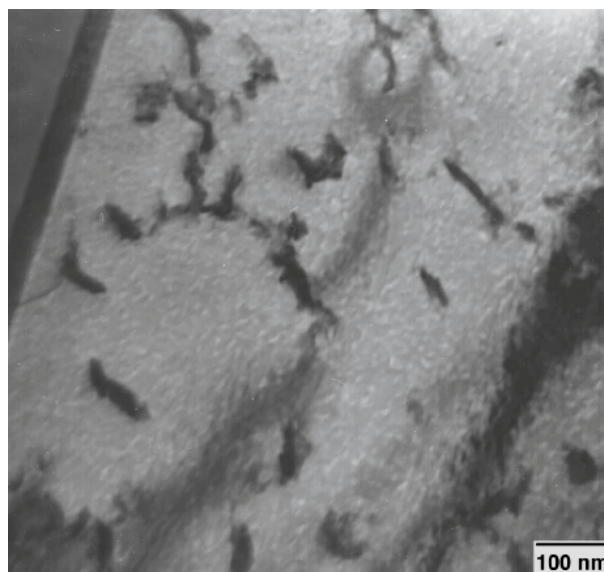


Fig. 16: 475°C – 1000 h tempered 25 Cr 7 Ni DSS microstructure TEM analysis; dislocations with precipitates in ferritic grain.

4. Conclusions

In this work, chemical composition influence on DSS “475°C embrittlement” phenomenon has been investigated both considering fatigue crack propagation resistance and analyzing microstructure transformations using a transmission electron microscope (TEM). Three different rolled DSS were investigated considering the same ferrite/austenite ratio:

- a “lean” duplex stainless steel 21Cr 1 Ni;
- a “classic” duplex stainless steel 22 Cr 5 Ni;
- a superduplex stainless steel 25 Cr 7 Ni.

Fatigue crack propagation results obtained considering both solubilized and 475°C-1000h tempered steels and TEM microstructure analysis, allowed to point out the following conclusions:

- 21 Cr 1 Ni seems to be characterized by the worst fatigue crack propagation resistance, if compared to the other two investigated DSS, but shows the lowest susceptibility to the 475°C embrittlement mechanism;
- Solubilized 22 Cr 5 Ni is characterized by the same fatigue crack propagation resistance that is offered by the SSS 25 Cr 7 Ni for all the investigated loading conditions;
- Both 22Cr 5 Ni DSS and 25 Cr 7 Ni are prone to be embrittled at 475°C after 1000 hours: influence on $da/dN-\Delta K$ curve is strongly influenced by chemical composition;
- Differences in the 475°C embrittlement susceptibility are due to the chemical composition influence on the G phase precipitation mechanism: higher content of G phase forming elements (Ni, Mo) implies larger G phase particles for the same permanence at 475°C; no evident differences were observed concerning the ferrite grains spinodal decomposition.

Acknowledgements

Outokumpu S.p.A. is warmly acknowledged.

References

- ASTM E647-15e1, 2015. Standard test method for measurement of fatigue crack growth rates.
 Charles, J., 2008. Duplex Stainless Steels - a Review after DSS '07 held in Grado, Steel Research International, 79, 455-465.

- Danoix, F., Auger, P., 2000. Atom probe studies of the Fe–Cr system and stainless steels aged at intermediate temperature: a review. *Materials Characterisation*, 44, 177201.
- Fruytier, D.J.A., 1991. Industrial experiences with duplex stainless steel related to their specific properties. *Duplex stainless steel '91*, Beaune, France, 1, 497-510.
- Gunn, R.N., 1997. *Duplex Stainless steels. Microstructure, properties and applications*. Abington Publishing, Cambridge, England.
- Guttman, M., 1991. Intermediate temperature aging of duplex stainless steels. A review. *Duplex stainless steel '91*, Beaune, France, 1, 79-92.
- Iacoviello, F., Habashi, M., Cavallini, M., 1997. Hydrogen embrittlement on the duplex stainless steel Z2CND2205 hydrogen charged at 200°C. *Materials Science and Engineering A*, A224, 116-124.
- Iacoviello, F., Galland, J., Habashi, M., 1998. A thermal outgassing method (T.O.M.) to measure the hydrogen coefficient of diffusion in austenitic and austeno-ferritic steels, *Corrosion Science*, 40, 1281-1293.
- Iacoviello, F., Boniardi, M., La Vecchia, G.M., 1999. Fatigue crack propagation in austeno-ferritic stainless steel 22 Cr 5 Ni. *Int. Journal of Fatigue*, 21, 957-963.
- Iacoviello, F., 2000. Statistical behaviour of ΔK threshold values and life prediction analysis in 2091 Al-Li alloy. *Int. J. of Fatigue*, 22, 657-663.
- Iacoviello, F., Casari, F., Gialanella, S., 2005. Effect of “475°C embrittlement” on duplex stainless steels localised corrosion resistance, *Corrosion Science*, 47, 909-922.
- Lacombe, P., Baroux, B., Beranger, G., 1990. *Les aciers inoxydables*, Les éditions de physique, Les Ulis Cedex A, France, 663.
- Nilsson, J.-O., 1992. Super duplex stainless steels. *Materials Science and Technology*, 8, 685-700.
- Park, C.J., Kwon, H.S. 2002. Effects of aging at 475 °C on corrosion properties of tungsten-containing duplex stainless steels *Corr. Science*, 44, 2817-2830.